HHS Public Access

Author manuscript

Exp Neurol. Author manuscript; available in PMC 2016 November 01.

Published in final edited form as:

Exp Neurol. 2015 November ; 273: 1–10. doi:10.1016/j.expneurol.2015.07.021.

Diffusion tensor imaging and myelin composition analysis reveal abnormal myelination in corpus callosum of canine mucopolysaccharidosis I

James M. Provenzale[1,2], **Igor Nestrasil**[3], **Steven Chen**[1], **Shih-hsin Kan**[4], **Steven Q. Le**[4], **Jacqueline K. Jens**[5], **Elizabeth M. Snella**[5], **Kristen N. Vondrak**[4], **Jennifer K. Yee**[4], **Charles H. Vite**[6], **David Elashoff**[7], **Lewei Duan**[7], **Raymond Y. Wang**[8], **N. Matthew Ellinwood**[5], **Miguel A. Guzman**[9], **Elsa G. Shapiro**[3], and **Patricia I. Dickson**[4,*]

[1]Duke University, Department of Radiology, Durham, NC, USA

[2]Emory University, Department of Radiology, Oncology & Biomedical Engineering, Atlanta, GA, USA

[3]University of Minnesota, Department of Pediatrics, Minneapolis, MN, USA

[4]Los Angeles Biomedical Research Institute at Harbor-UCLA Medical Center, Department of Pediatrics, Torrance, CA, USA

[5]Iowa State University, Department of Animal Science, Ames, IA, USA

[6]University of Pennsylvania School of Veterinary Medicine, Department of Clinical Studies, Philadelphia, PA, USA

[7]University of California, Los Angeles, Departments of Medicine and Biostatistics, Los Angeles, CA, USA

[8]Children's Hospital Orange County, Orange, CA, USA

[9]Saint Louis University School of Medicine, Department of Pathology, Saint Louis, MO, USA

Abstract

Children with mucopolysaccharidosis I (MPS I) develop hyperintense white matter foci on T2-weighted brain magnetic resonance (MR) imaging that are associated clinically with cognitive impairment. We report here a diffusion tensor imaging (DTI) and tissue evaluation of white matter in a canine model of MPS I. We found that two DTI parameters, fractional anisotropy (a measure of white matter integrity) and radial diffusivity (which reflects degree of myelination) were

*To whom correspondence should be addressed: Patricia I. Dickson, M.D., 1124 W. Carson St, HH1, Torrance, CA 90502 U.S.A., +1 310 781 1399, pdickson@ucla.edu.

Conflicts of interest: The Los Angeles Biomedical Research Institute at Harbor-UCLA Medical Center and the Department of Pediatrics at Harbor-UCLA (but not the authors) receive royalties from the sale of recombinant human alpha-L-iduronidase (laronidase). P.I.D., E.G.S. and N.M.E. receive research support from, and R.Y.W. has received travel support and served as a consultant for, BioMarin and/or Genzyme-Sanofi, which manufacture and distribute laronidase.

abnormal in the corpus callosum of MPS I dogs compared to carrier controls. Tissue studies of the corpus callosum showed reduced expression of myelin-related genes and an abnormal composition of myelin in MPS I dogs. We treated MPS I dogs with recombinant alpha-L-iduronidase, which is the enzyme that is deficient in MPS I disease. The recombinant alpha-L-iduronidase was administered by intrathecal injection into the cisterna magna. Treated dogs showed partial correction of corpus callosum myelination. Our findings suggest that abnormal myelination occurs in the canine MPS I brain, that it may underlie clinically-relevant brain imaging findings in human MPS I patients, and that it may respond to treatment.

Keywords

diffusion tensor imaging; neuroimaging; Hurler; Scheie; enzyme replacement therapy; lysosomal storage disease; anisotropy; brain

Introduction

MPS I (a.k.a. “Hurler syndrome) is an inherited disease that causes progressive loss of cognitive function and substantial physical disease in children. In MPS I, glycosaminoglycans accumulate intracellularly, due to the deficiency of the lysosomal enzyme alpha-L-iduronidase. However, glycosaminoglycans are not directly toxic, and the cause of neurological deterioration in children with MPS I is not presently clear. Brain histological findings in MPS I patients have shown neuronal cell loss, gliosis, swelling of cell bodies and dendrites, prominent perivascular (i.e., Virchow-Robin) spaces, leptomeningeal thickening, and gross atrophy (Naidoo, 1953). In addition, brain MR imaging findings show hydrocephalus, cribriform changes, and hyperintense lesions of white matter (Seto et al., 2001). Some investigators have speculated that the hyperintense lesions of white matter are caused by abnormal myelination (Gabrielli et al., 2004). In this study, we performed a controlled, preclinical study of MPS I and carrier control dogs to determine whether white matter abnormalities described in human MPS I could be detected in MPS I dogs. Canine studies are essential because humans affected with severe MPS I disease typically receive bone marrow transplantation and immune suppression therapy, which could confound observational imaging studies and studies of novel therapies.

In previous studies, we used a naturally-occurring canine model of MPS type I to study the neurological disease due to MPS I and its potential treatment (Dierenfeld et al., 2010; Shull et al., 1982; Vite et al., 2013). In one study, we used MR imaging to assess anatomic and structural features of the brains of three canine populations: nine adult MPS I dogs, four age-matched, unaffected carrier dogs and four MPS I dogs that had been treated beginning at four months of age with intrathecal recombinant human alpha-L-iduronidase at three month intervals (Vite et al., 2013). The study showed that the canine MPS I brain shares many anatomic features with human MPS I disease including ventriculomegaly, brain cortical atrophy, and volume loss in the corpus callosum that was prevented by treatment (Vite et al., 2013). The neuroimaging findings of volume loss in the corpus callosum (a major white matter structure) and hyperintense regions within the white matter suggested the possibility of white matter involvement, including demyelination. With this in mind, we set out to study

brain microstructure in MPS I dogs using MR techniques that would reflect myelination changes on the microscopic level and correlate those findings with the composition of myelin and expression of myelin-related genes.

DTI is a MR technique that provides information about the microstructure of white matter through measurement of the microscopic, three-dimensional motion of water. DTI studies of the brain in MPS I children have shown reduced fractional anisotropy (FA) in the corpus callosum, a finding that has been correlated with reduced attention and suggests that abnormalities within white matter may underlie some aspects of the loss of function in MPS I patients (Shapiro et al., 2012). Another pertinent DTI metric is radial diffusivity, which has been shown to correlate with absence of myelination (Song et al., 2002).

In the present study, we set out to correlate DTI findings and features of demyelination of the same dogs that were examined in our previous study. Our first hypothesis was that both FA values and RD values would be altered in the white matter of untreated MPS I dogs. Our second hypothesis was that these findings would correlate with degree of myelination (as measured by levels of myelin basic protein (MBP) as well as altered myelin composition and diminished expression of myelin-related genes). Our third hypothesis was that treatment with intrathecal recombinant human alpha-L-iduronidase would ameliorate both the altered DTI metrics and the pre-existent defects in myelin composition and gene expression. Finding of a correlation between DTI parameters and a quantitative measurement of degree of myelination is very important if DTI is to be useful as a means to measure therapeutic response in demyelinating diseases. As a representative white matter structure, we chose the corpus callosum, a highly anisotropic structure that is easily identified in the canine brain.

Materials and Methods

Study design

Research objectives—We performed a controlled, preclinical study of MPS I and carrier control dogs to determine whether white matter abnormalities described in human MPS I could be detected in MPS I dogs. Canine studies were essential, because patients affected with severe MPS I disease typically receive bone marrow transplantation and immune suppression which could confound observational imaging studies in human subjects. Following our initial determination of reduced fractional anisotropy in the corpus callosum of affected dogs vs. controls, we performed further data and tissue analyses to determine whether the changes reflected abnormal myelination. We also studied treated MPS I dogs to determine whether the imaging and compositional abnormalities that we discovered would respond to therapeutic intervention.

Research subjects—Dogs were bred from the original Plott hound colony (Shull et al., 1982). Study subjects were maintained in accordance with US Department of Agriculture and NIH guidelines for the care of dogs. All study procedures were reviewed and approved by institutional animal care and use committees. Dogs were bred and maintained as described (Vite et al., 2013). We used a mix of heterozygous and homozygous normal control dogs from this kindred. Heterozygous dogs are carriers only and have never been documented to have manifestations of MPS I disease at any time. The dogs in this study

were previously described with respect to their brain magnetic resonance imaging findings (Vite et al., 2013).

Experimental design—Treated dogs (both genders) received recombinant human alpha-L-iduronidase (formulated as laronidase, BioMarin Pharmaceutical, Novato, CA). For intrathecal treatment, 0.05 mg/kg body weight (up to 1 mg) recombinant human alpha-L-iduronidase was diluted in 1:2 (v/v) Elliotts B artificial spinal fluid (DRAXIS Pharma, Kirkland, Quebec, Canada) and administered into the cisterna magna at three month intervals as previously described (Vite et al., 2013). Four of the nine untreated MPS I dogs (I-371, I-388, I-392 and I-393) received intra-articular treatment with 1 mg recombinant human alpha-L-iduronidase to the right stifle (knee) and elbow joints once monthly for six months in a separate study (Wang et al., 2014). Intra-articular treatment would not be expected to affect MPS disease in the brain. Dogs received 2.2 mg/kg diphenhydramine prior to intrathecal recombinant human alpha-L-iduronidase administration to prevent infusion reactions.

Sample size—We used heterozygous normal control dogs from this kindred for this study. Heterozygous dogs are carriers only and are not expected, and have never been documented in the over 30 years that the model has existed at five different sites, to have manifestations of MPS I disease at any time. Animals of this kindred are preferred controls relative to other wildtype dogs from outside of the colony (which could have other genetic variations). Sample size was determined mainly by availability of animals. However, we estimated that there is a 25% reduction in fractional anisotropy of the corpus callosum in human MPS I patients compared to controls. Power analysis suggests that four animals per group would yield >97% power to detect a 25% change with an estimated SD of 10%.

Data inclusion and outliers—No animals were lost during the study, and data from all animals were included. No data were treated as outliers. Two neuroimaging studies with high levels of artifact (such as motion artifact) were identified, not analyzed, and excluded from the data set. Since with one exception at least two and in some cases three scans were performed for each animal, we were able to include imaging studies for each dog in the results. More information about excluded imaging studies can be found below under “DTI.”

Endpoints and experimental replicates—DTI endpoints were prospectively determined (FA, radial and axial diffusivity, and ADC). For all results, except where noted we used Bonferroni correction for multiple comparisons. Each animal was an experimental replicate, except for RT-PCR where plates were experimental replicates. Dogs were scanned twice, and if both scans were acceptable then both were analyzed and the results averaged. Assays were performed in triplicate and the means reported.

Randomization and blinding—Randomization was not performed in this exploratory study. Blinding to MPS and treatment status was performed for all outcome measures.

DTI

Dogs were imaged using a 3.0-Tesla scanner (Discovery MR 750, GE Healthcare, Little Chalfont, United Kingdom) and an 8-channel transmit–receive knee coil. DTI was performed with an axial single-shot echo-planar imaging sequence containing 37 slices aligned to the anterior and posterior commissures. The acquisition parameters were TR/TE 6,000/86 ms, flip angle 90°, slices thickness of 1.5 mm, no gap, 4 NEX, matrix of 128 × 128. Three volumes with diffusion weighting b-factor of 0 s/mm^2 and 25 volumes with b-factor of 1000 s/mm^2 were acquired. We also performed anatomical imaging, as previously published (Vite et al., 2013). Anesthesia was managed as previously described (Vite et al., 2013).

In general, an attempt was made to perform MR imaging on each dog twice, at one week intervals. All dogs except two were imaged twice during that time interval. One carrier dog was scanned once and one untreated MPS dog was scanned three times. DTI imaging was acceptable in all but one of the 7 DTI scans performed in the carrier dogs, all but one of the 9 DTI scans performed in the untreated MPS dogs, and in all 18 DTI scans performed in treated dogs.

DICOM-formatted images were first processed using the DtiStudio software suite (Johns Hopkins University, Baltimore, MD) (Jiang et al., 2006). All images were first inspected for the presence of artifacts. A B_0 correction was performed on the raw diffusion-weighted images using automated image registration in DtiStudio to correct for eddy currents and motion. We performed a linear transformation in DiffeoMap using a twelve-parameter affine approach with a trilinear interpolation on the axial proton density image using the FA map as the template for the purpose of anatomical localization. The fractional anisotropy (FA), apparent diffusion coefficient (ADC), axial diffusivity ($\lambda 1$), and radial diffusivity ([$\lambda 2$ + $\lambda 3$]/2) maps were then derived.

We used the fiber assignment by continuous tracking (FACT) algorithm in DtiStudio 3.0.2 for tractography (Mori et al., 1999). We set FA thresholds to 0.2 to initiate and continue tracking; the maximum angle threshold was 0°. We used a single region-of-interest (ROI) approach for tractography of the genu and splenium of the corpus callosum.

Relationship between MBP Levels and DTI Metrics

To determine the relationship between myelination and DTI, we quantified MBP using a sandwich ELISA. We then performed linear regression analysis of FA, radial diffusivity, axial diffusivity, and ADC using MBP as the independent variable (Fig. 2C). A subset of dogs representing all three groups was included in the analysis. This set included 4 untreated MPS dogs, 2 MPS dogs treated with intrathecal recombinant alpha-L-iduronidase (MTr) dogs, and 4 normal carrier (CTL) dogs and was limited by available tissue for quantitative MBP analysis.

Expression of Myelin-Related Genes

We isolated total RNA from canine corpus callosum (genu and splenium) using an RNeasy Lipid Tissue Kit (QIAGEN, Valencia, CA) and performed semi-quantitative real-time

reverse transcriptase-polymerase chain reaction (RT-PCR) analysis. We measured the total RNA quantity with NanoDrop (Thermo Scientific, Wilmington, DE). We synthesized cDNA from ~100–500 ng of RNA using the AffinityScript cDNA Synthesis kit (Agilent Technologies, Santa Clara, CA) with random hexamer primers, according to the manufacturer's instructions. The resulting cDNA was diluted 10-fold, and a 2-μl aliquot was used in a 10-μl PCR reaction (Power SYBR Green, Life Technology, Carlsbad, CA) containing primers at a concentration of 100 nM each. PCR reactions were run in triplicate and quantified in the ABI 7,900HT Sequence Detection System. We normalized cycle threshold (C_T) values to peptidylprolyl isomerase A (*PPIA*) expression (Fletcher et al., 2011) and expressed the results as fold-change of mRNA compared to control canine samples. Primers were optimized over exon-exon junctions to a calculated T_m of 60 °C and synthesized by Eurofins MWG Operon (Huntsville, AL). The myelinrelated genes that we evaluated included *MAL* (myelin and lymphocyte protein), *PLP1* (proteolipid protein 1), *MBP* (myelin basic protein), *MAG* (myelin associated glycoprotein), *MOG* (myelin oligodendrocyte glycoprotein), and *MOBP* (myelin-associated oligodendrocyte basic protein). Primer sequences were: *MAL* forward 5′-CGG ACC TGC TCT TCA TCT TC-3′ and *MAL* reverse 5′-AAC ACA GAC ACA AAC ATC ACC C-3′, *PLP1* forward 5′-CTG GCT GAG GGC TTC TAC AC-3′ and *PLP1* reverse 5′-CAG CAG AGC AGG CAA ACA C-3′, *PPIA* forward 5′-ATG GAT GGC GAG CCT TTG-3′ and *PPIA* reverse 5′-CTT TTC CCC GTA GAT GGA CTT G-3′, *MBP* forward 5′-GGA CTG TCC CTC AGC AGA TT-3′ and *MBP* reverse 5′-CTT GAG CCC CTT GTG AGC-3′, *MAG* forward 5′-TCA TTG CCA TCG TCT GCT AC-3′ and *MAG* reverse 5′-TCA CTG CTG AAC AGG ACA GG-3′, *MOG* forward 5′-GTC CAT GGA GCT CCT CTC TG-3′ and *MOG* reverse 5′-GAG TGG GTG ACC TGG TCC TA-3′, *MOBP* forward 5′-AAA AGT GGC TGC TTC TAC CAG-3′ and *MOBP* reverse 5′-CTC TGA GGG GAC GTT GCA C-3′. PCR was performed in triplicate and the data analyzed using $2^{-\Delta\Delta C_T}$ (Livak and Schmittgen, 2001).

Myelin Composition

To evaluate the composition of white matter myelin in MPS I dogs, we dissected the corpus callosum from MPS I and carrier control dogs and isolated the genu and splenium. We extracted the myelin from the genu and splenium using sucrose gradient centrifugation (Norton Wt and Poduslo, 1973). The main components of myelin are protein and lipids. We examined composition of white matter myelin in two ways. First, we measured the protein concentration of myelin. Next, we measured the composition of white matter myelin by measuring myelin basic protein.

For western blots, we loaded 1.5 μg protein of homogenate (of extracted myelin) onto 4–20% Tris-Glycine protein gels (Life Technology) and probed the blot with antibodies against myelin basic protein and actin (EMD Millipore, Billerica, MA). For quantitative measurement of myelin basic protein, we performed sandwich ELISA by coating 96-well plates with rat polyclonal anti-myelin basic protein antibody (82–87; EMD Millipore), adding 50 μl (1:50 dilution) extracted myelin to each well, applying mouse monoclonal anti-myelin basic protein antibody (119–131; EMD Millipore), goat anti-mouse secondary antibody (alkaline phosphatase-conjugated; Southern Biotech, Birmingham, AL), and developing with pNPP substrate (Sigma-Aldrich, St. Louis, MO). Samples were read using a

Biotek plate reader (Synergy-2, Biotek, Winooski, VT) at 405 nm. Bovine myelin basic protein (EMD Millipore) was used to establish a standard curve.

Evaluation of Lipidomics

For lipid analysis, myelin underwent sequential extraction with chloroform methanol (1:2), chloroform and water (1:1), then chloroform alone (Welti et al., 2007). Finally, we washed the lower layers containing the lipid in 1 M KCl and water. Aliquots of ~9 μg lipid (estimated based on original myelin protein concentrations) taken from each sample underwent liquid chromatography/tandem mass spectrometry (LCMSMS) analysis by the Kansas Lipidomics Research Center using previously published methods. One aliquot was analyzed for polar lipids on an API 4000™ (ABSciex, Framingham, MA), while a second aliquot was analyzed for ceramides and hexosylceramides on a 4000 Q-Trap® (ABSciex) (Devaiah et al., 2006; Welti et al., 2007). Lipid signals were normalized to protein content (nmol/mg protein for polar lipids, and signal/mg protein for ceramides and hexosylceramides). For the ceramide and hexosylceramide analysis, species in which the fatty acid carbon chain was no longer than 26 were identified (these are the species most likely found in brain), and the spectral peaks representing ions with or without loss of water molecules were added together. We assayed cholesterol (total) using the Amplex Red assay kit (Life Technology). We measured esterified cholesterol by adding myelin extraction samples to a 96-well plate and applying reagents mix of cholesterol esterase, cholesterol oxidase, amplex red, and horseradish peroxidase provided by the kit. We incubated samples and reagents at 37 °C for 30 min in a Biotek plater reader (Synergy-2) and read them at excitation 530 nm and emission 590 nm. We created a standard curve for cholesterol using cholesterol provided in the kit. We measured protein in myelin extracts using the Bradford protein assay (Bio-Rad, Hercules, CA). Results from genu and splenium were similar and were averaged for each *animal*.

Statistical Analysis

For comparisons of DTI metrics and MBP content, we used linear regression (least-squares method; SYSTAT13, Systat, Chicago, IL) to compare the dependent variables FA, ADC, radial diffusivity and axial diffusivity versus the independent variable, MBP. Each animal was an experimental replicate.

For the statistical analysis of myelin composition (except for lipidomics), SigmaPlot 12 and SYSTAT 13 statistical software (Systat, Chicago, IL) were used for graphing and statistical analysis, respectively. We analyzed data using ANOVA with Tukey-Kramer *post-hoc* test. Each animal was an experimental replicate. Except where noted, we used Bonferroni correction to adjust the confidence interval for multiple comparisons.

Lipidomics analyses were performed in R version 2.14.0. The primary outcome measures were the quantities of polar lipid, ceramide and hexosylceramide classes, and individual lipid species, normalized to protein content (nmol or signal/mg protein). The percent of total signal (not normalized to protein) for each polar lipid class was also analyzed to examine lipid composition in parallel with lipid quantities. Data was filtered to include only lipid compounds with at least 3 non-zero values in at least one of the groups. For polar lipids, the

raw data included 352 compounds, and 260 compounds remained after filtering. After assessment for normal distribution of data, we compared lipid variables among the three groups using ANOVA. We performed pair-wise t-tests using a pooled standard deviation estimate across all groups with Bonferroni adjustment for multiple comparisons to compare each pair of groups in cases in which the overall ANOVA test was significant. We performed principal components analyses separately for the set of polar lipids and the set of ceramide and hexosylceramide classes. The first principal component was plotted versus the second principal component to assess whether the information from the set of classes could separate the groups. Next, we performed hierarchical clustering on the standardized percentages for both polar lipid species and for ceramides/hexceramides. We used R package "qvalue" for q value estimation, "cluster," "lattice," "gclus," "MASS," and "calibrate" for PCA analysis, and "pls" to standardize matrix for heatmap production. We set statistical significance to 0.05.

Results

DTI suggests abnormal myelination in MPS I dogs

The study subjects are listed in Table 1. DTI demonstrated a 20–30% decrease in fractional anisotropy and an increase in radial diffusivity of up to 63% higher in the corpus callosum of MPS I dogs compared to carrier controls ($P < 0.01$; Fig. 1 and Table 2). Mean FA value in the genu of the corpus callosum in heterozygous (i.e., control) dogs was 0.437 and that in the splenium was 0.514. In comparison, mean value in the genu of untreated affected dogs was 0.348 and in the splenium was 0.361. These differences were statistically significant. Treated MPS dogs had a mean FA value of 0.402, a mean ADC value of 9.18×10^{-4} and a mean RD value of 7.17×10^{-4} in the genu and a mean FA value of 0.430, a mean ADC value of 9.12×10^{-4} and a mean radial diffusivity value of 6.84×10^{-4} in the splenium (Table 2). The values in treated dogs were intermediate between the same values in the untreated MPS dogs and controls, but these differences did not meet statistical significance. Similarly, in untreated affected dogs, elevated radial diffusivity values, consistent with impaired myelination, were seen in the genu of (mean 8.60×10^{-4}) and splenium (mean 9.10×10^{-4}) of corpus callosum compared to the genu (mean 6.66×10^{-4}) and splenium (mean 5.60×10^{-4}) of control dogs, which did not meet statistical significance.

Relationship between MBP levels and DTI Metrics

Western blot samples and sandwich ELISA demonstrated diminished myelin basic protein in purified myelin fractions from the corpus callosum of affected dogs ($P = 0.004$), which was not markedly improved in treated dogs (Fig. 2A, B. Fractional anisotropy and radial diffusivity showed a linear relationship with MBP in the corpus callosum, suggesting an association between imaging findings and corpus callosum myelination (Fig. 2C). We found a linear relationship between FA and MBP in both the genu and splenium of the corpus callosum ($R^2 = 0.51$, Standardized Regression Coefficient (β_1) =0.7, p = 0.02 for genu; $R^2 = 0.83$, $\beta_1 = 0.9$, $p < 0.001$ for splenium). A negative relationship was seen between radial diffusivity and MBP in the genu of the corpus callosum ($R^2 = 0.51$, $\beta_1 = -0.7$, p = 0.02 for genu; $R^2 = 0.12$, $\beta_1 = -0.3$, p = NS in splenium). ADC values also tended to decrease with increasing MBP levels in the genu, but results did not reach statistical significance (Fig. 2C;

$R^2 = 0.39$, $\beta_1 = -0.6$, p = 0.05 for genu; $R^2 = 0.01$, $\beta_1 = 0.1$, p = NS for the splenium). We found no relationship between axial diffusivity and MBP (Fig. 2C; $R^2 = 0.25$, p = NS for genu; $R^2 = 0.29$, p= NS for splenium).

Evaluation of Myelin Composition and Gene Expression

RT-PCR of corpus callosum showed reduced expression of myelin-related genes in MPS I dogs compared to controls (Fig. 3A). Gene expression was not improved in adult MPS I dogs that had been treated from 4 months to 21 months of age with intrathecal recombinant human alpha-L-iduronidase.

The protein concentration of myelin extracted from MPS I dogs was reduced compared to carrier controls ($P = 0.005$) and was higher in MPS I dogs treated with intrathecal recombinant human alpha-L-iduronidase than it was in either untreated MPS I dogs or carrier controls ($P < 0.001$; Fig. 3B). We have previously found high concentrations of iduronidase in the corpus callosum of treated dogs, which may explain their elevated protein levels in myelin (Vite et al., 2013). Total cholesterol (normalized to protein concentration) was higher in myelin extracts from MPS I dogs compared to carrier controls ($P = 0.005$; Fig. 3C). However, cholesterol values were not improved in MPS I dogs treated with intrathecal recombinant human alpha-L-iduronidase. Most cholesterol in myelin is normally unesterified, and we found this to be the case in MPS I and carrier dogs.

Lipidomics Analysis

Total polar lipid content (which includes phospholipids) was studied by liquid chromatography/tandem mass spectrometry (LCMSMS) analysis. MPS I dogs exhibited significantly lower sphingomyelin and dihydrosphingomyelin ($P < 0.01$), and phosphatidylserine (PS) levels ($P = 0.01$; Fig. 4A and Table 3). There was a trend to low total polar lipid content in MPS I dogs compared to controls ($P = 0.06$), and no difference in ceramide and hexasoylceramide content. Hexasoylceramides comprised 92 ± 1% of the ceramide and hexasoylceramide lipids of corpus callosum myelin. Lipid composition analysis (Fig. 4B) showed normal proportions of PS, but a high proportion of phosphatidylethanolamine (PE) in MPS I. The findings suggest the possibility that PS in MPS I may undergo increased turnover to PE, possibly to maintain substrate supply for downstream phosphatidylcholine synthesis. In MPS I dogs, ceramides were 24 ± 7% lower ($P = 0.01$), but hexosylceramides were not significantly lower compared to controls (Table 4). Principal components analyses (Fig. 5, A and B) of polar, ceramide and hexosylceramide lipids showed separation of MPS I treated and untreated groups. Principal components 1 and 2 by polar lipid species (Fig. 5A) accounted for 54% of the variance, which was largely influenced by sphingomyelin and dihydrosphingomyelin, phosphatidylserine, and ether-linked phosphatidylserine species. Principal components analysis by ceramide and hexasoylceramide species (Fig. 5B) showed that principal components 1 and 2 accounted for 60% variance, which was influenced by long chain ceramide and hexasoylceramide species, including ceramide d18:1-26:0-O, hexasoylceramide d18:1-24:0-O, and hexasoylceramide d18:1-26:0-O. Heatmap analyses (Fig. 5, C and D) demonstrated overlap among the MPS I treated and untreated groups, consistent with the lack of restoration of many polar lipid species despite treatment (Table 3).

Discussion

In this investigation, we proposed three study hypotheses. Our first hypothesis was that both FA values and radial diffusivity values would be altered in the white matter of untreated MPS I dogs. Our second hypothesis was that DTI findings would correlate with altered myelin composition and diminished expression of myelin-related genes. Third, we hypothesized that intrathecal recombinant human alpha-L-iduronidase treatment would ameliorate both the effects of the disease on myelin composition and gene expression and the altered DTI features.

One important aspect of our study is the histological confirmation of DTI changes seen in our study population. Correlations of DTI metrics and quantitative histological observations are especially important for determining the value of DTI as a noninvasive means of assessment of therapeutic response. A number of studies have used DTI to follow serial changes in the brain after therapy (McGraw et al., 2005). However, few studies have validated DTI metrics by providing histological correlates of the major DTI parameters, such as FA and radial diffusivity (Song et al., 2002; Wei et al., 2013). One investigator has previously shown that radial diffusivity, but not FA, correlated with degree of demyelination based on Luxol fast blue-stained slides of spinal cord derived from multiple sclerosis patients (Klawiter et al., 2011), However, unlike our study, that investigation was based on a semi-quantitative grading system for degree of demyelination (rather than on a quantitative analysis of myelin content) and also did not measure response to a treatment. In our study, which used a measurement of myelin basic protein as a quantitative metric of degree of demyelination, we found that both radial diffusivity and FA correlated with degree of demyelination in a significant manner.

Our neuroimaging and neuropathology studies of the corpus callosum in MPS I dogs suggest that significant diminution of myelination occurs in the disease, the composition of the myelin is abnormal, and myelin-related genes are under-expressed. Reduced expression of myelin-related genes have also been found in the brains of animal models with other types of MPS (DiRosario et al., 2009; Parente et al., 2012). We did not investigate the underlying cause of abnormal myelination. Thus we cannot determine whether MPS I dogs have a primary problem with myelin, or whether the abnormal myelination that we observed is secondary to neuronal loss or other factors. One potential mechanism for the disordered myelin in MPS I is accumulation of heparan sulfate, which has been reported to block the maturation of oligodendrocyte precursors (Sloane Ja et al., 2010). Further studies are also needed to determine whether myelin forms abnormally, or alternatively, becomes abnormal over time with progression of MPS disease.

Recombinant human alpha-L-iduronidase is normally administered to human patients with MPS I intravenously. In the present study, we provided an intrathecal method of infusion that allowed the enzyme to bypass the blood-brain barrier and which may have resulted in improved brain delivery. We administered therapy relatively infrequently (at three-month intervals). This frequency is supported by previous studies of intrathecal recombinant alpha-L-iduronidase in MPS I dogs (Dickson et al., 2007). While we did see a partial correction in DTI metrics and myelin composition in treated animals, these changes were incomplete and

did not reach statistical significance. The late age at which the animals initiated treatment may have affected our ability to completely correct MPS I disease. Our previous research indicates that treatment within the first month of life is highly effective for prevention of brain lysosomal storage in the canine model of MPS I (Dierenfeld et al., 2010). MPS I dogs also mount an antibody response to intrathecally-administered recombinant human alpha-L-iduronidase that can reduce its ability to correct the biochemical phenotype (Dickson et al., 2012).

Like any study, our investigation is subject to a number of limitations. First, relatively small numbers of dogs of mixed gender were used. In addition, we did not perform serial imaging of dogs in a manner that would allow determination the exact onset and course of abnormal myelination. Furthermore, our studies focused only on the corpus callosum; we recognize that different findings might be seen in other white matter structures. The signal-to-noise ratio afforded by our imaging technique did not allow us to confidently measure DTI metrics in smaller white matter tracts using tractography. We expect that future refinements to our methodology and imaging acquisitions may permit accurate analysis of other white matter structures. While we found an overall relationship between DTI metrics and MBP values in the dogs, we were unable to evaluate this relationship within each subgroup of dogs (for example, solely untreated MPS I dogs), due to insufficient numbers of animals. Finally, because MPS I dogs develop hydrocephalus, the resultant anatomic distortion of the corpus callosum may confound DTI studies of the corpus callosum and may even contribute to abnormalities in myelin (Hanlo et al., 1997; Zimmerman et al., 1986).

We used a large animal model to investigate a clinical observation (the correlation of functional impairment with reduced fractional anisotropy of the corpus callosum in children with MPS I, (Shapiro et al., 2012). Our findings have potential implications for the study and treatment of MPS disorders. If abnormal myelination contributes substantially to the MPS phenotype, then our results indicate a potential avenue for development of new therapies. Also, if increased radial diffusivity in the corpus callosum does indeed reflect abnormal myelin as we suspect, then DTI would allow us to quantify it in a non-invasive way, which may be relevant for prognosis and therapeutic response. Our research may also point to the development of myelin-related biomarkers in cerebrospinal fluid as a way of monitoring disease progression and response to therapy. For this rare disease in which controlled, natural history studies are challenging, the canine model may provide a way to investigate potential clinical markers for disease relevance prior to their application to human subjects.

Acknowledgements

Catalina Guerra, Jenny Dancourt, and Amanda Todd at the Los Angeles Biomedical Research Institute at Harbor-UCLA Medical Center, and numerous undergraduate students at Iowa State University, provided assistance with animals. Carolyn Sinow and Megan Craig assisted with axon counts on EM images. Daisy O'Brien and Shida Banakar operated the MRI scanner. Leonard White assisted with neuroanatomy. Funding was provided by NIH/NINDS NS085381 and NS05242 to P.I.D., T32 GM8243-27 to support S.-h.K., NIH/NCATS (UCLA CTSI) UL1TR000124, NIH/NIBIB (Duke Center for In Vivo Microscopy) P41 EB015897 to G. Allan Johnson, NIH/OD P40 OD010939 to Mark Haskins and NIH/NIDDK R01 DK066448 to Katherine Ponder, and grants from the Ryan Foundation and the Gene Spotlight Charity Inc. to N.M.E. Lipid analysis was performed at the Kansas Lipidomics Research Center (KLRC). Mary Roth and Ruth Welti of the KLRC provided advice regarding data interpretation. Instrument acquisition and method development at KLRC was supported by NSF grants MCB 0455318 and

0920663 and DBI 0521587, and NSF EPSCoR grant EPS-0236913 with matching support from the State of Kansas through Kansas Technology Enterprise Corporation and Kansas State University. The KLRC is also supported by K-INBRE (NIH Grant P20 RR16475 from the INBRE program of the National Center for Research Resources). Canine care and housing was also supported in part by grants from the MPS1 Research Foundation and CHOC Pediatric Subspecialty Faculty to R.Y.W. Recombinant human alpha-ʟ-iduronidase was provided by BioMarin Pharmaceutical Inc.

References

Devaiah SP, Roth MR, Baughman E, Li M, Tamura P, Jeannotte R, Welti R, Wang X. Quantitative profiling of polar glycerolipid species from organs of wild-type Arabidopsis and a PHOSPHOLIPASE Dα1 knockout mutant. Phytochemistry. 2006; 67:1907–1924. [PubMed: 16843506]

Dickson P, McEntee M, Vogler C, Le S, Levy B, Peinovich M, Hanson S, Passage M, Kakkis E. Intrathecal enzyme replacement therapy: successful treatment of brain disease via the cerebrospinal fluid. Mol Genet Metab. 2007; 91:61–68. [PubMed: 17321776]

Dickson PI, Ellinwood NM, Brown JR, Witt RG, Le SQ, Passage MB, Vera MU, Crawford BE. Specific antibody titer alters the effectiveness of intrathecal enzyme replacement therapy in canine mucopolysaccharidosis I. Mol. Genet. Metab. 2012; 106:68–72. [PubMed: 22402327]

Dierenfeld AD, McEntee MF, Vogler CA, Vite CH, Chen AH, Passage M, Le S, Shah S, Jens JK, Snella EM, Kline KL, Parkes JD, Ware WA, Moran LE, Fales-Williams AJ, Wengert JA, Whitley RD, Betts DM, Boal AM, Riedesel EA, Gross W, Ellinwood NM, Dickson PI. Replacing the enzyme α-l-iduronidase at birth ameliorates symptoms in the brain and periphery of dogs with mucopolysaccharidosis type I. Sci. Transl. Med. 2010; 2:60ra89–60ra89.

DiRosario J, Divers E, Wang C, Etter J, Charrier A, Jukkola P, Auer H, Best V, Newsom DL, McCarty DM, Fu H. Innate and adaptive immune activation in the brain of MPS IIIB mouse model. J. Neurosci. Res. 2009; 87:978–990. [PubMed: 18951493]

Fletcher JL, Kondagari GS, Wright AL, Thomson PC, Williamson P, Taylor RM. Myelin genes are downregulated in canine fucosidosis. Biochim. Biophys. Acta - Mol. Basis Dis. 2011; 1812:1418–1426.

Gabrielli O, Polonara G, Regnicolo L, Petroni V, Scarabino T, Coppa GV, Salvolini U. Correlation between cerebral MRI abnormalities and mental retardation in patients with mucopolysaccharidoses. Am. J. Med. Genet. Part A. 2004; 125A:224–231. [PubMed: 14994229]

Hanlo PW, Gooskens RJHM, van Schooneveld M, Tulleken CAF, van der Knaap MS, Faber JAJ, Willemse J. The effect of intracranial pressure on myelination and the relationship with neurodevelopment in infantile hydrocephalus. Dev. Med. Child Neurol. 1997; 39:286–291. [PubMed: 9236693]

Jiang H, van Zijl PCM, Kim J, Pearlson GD, Mori S. DtiStudio: resource program for diffusion tensor computation and fiber bundle tracking. Comput. Methods Programs Biomed. 2006; 81:106–116. [PubMed: 16413083]

Klawiter EC, Schmidt RE, Trinkaus K, Liang H-F, Budde MD, Naismith RT, Song S-K, Cross AH, Benzinger TL. Radial diffusivity predicts demyelination in ex vivo multiple sclerosis spinal cords. Neuroimage. 2011; 55:1454–1460. [PubMed: 21238597]

Livak KJ, Schmittgen TD. Analysis of Relative Gene Expression Data Using Real-Time Quantitative PCR and the 2-[Delta][Delta]CT Method. Methods. 2001; 25:402–408. [PubMed: 11846609]

McGraw P, Liang L, Escolar M, Mukundan S, Kurtzberg J, Provenzale JM. Krabbe Disease Treated with Hematopoietic Stem Cell Transplantation: Serial Assessment of Anisotropy Measurements--Initial Experience. Radiology. 2005; 236:221–230. [PubMed: 15987975]

Mori S, Crain BJ, Chacko VP, van Zijl PC. Three-dimensional tracking of axonal projections in the brain by magnetic resonance imaging. Ann. Neurol. 1999; 45:265–269. [PubMed: 9989633]

Naidoo D. Gargoylism (Hurler's Disease): A neuropathological report. Br. J. Psychiatry. 1953; 99:74–83.

Norton Wt FAU, Poduslo SE. Myelination in rat brain: method of myelin isolation. J Neurochem. 1973; 21:749–757. [PubMed: 4271082]

Parente MK, Rozen R, Cearley CN, Wolfe JH. Dysregulation of gene expression in a lysosomal storage disease varies between brain regions implicating unexpected mechanisms of neuropathology. PLoS One. 2012; 7:e32419. [PubMed: 22403656]

Seto T, Kono K, Morimoto K, Inoue Y, Shintaku H, Hattori H, Matsuoka O, Yamano T, Tanaka A. Brain magnetic resonance imaging in 23 patients with mucopolysaccharidoses and the effect of bone marrow transplantation. Ann. Neurol. 2001; 50:79–92. [PubMed: 11456314]

Shapiro E, Guler OE, Rudser K, Delaney K, Bjoraker K, Whitley C, Tolar J, Orchard P, Provenzale J, Thomas KM. An exploratory study of brain function and structure in Mucopolysaccharidosis Type I: Long term observations following hematopoietic cell transplantation (HCT). Mol. Genet. Metab. 2012; 107:116–121. [PubMed: 22867884]

Shull RM, Munger RJ, Spellacy E, Hall CW, Constantopoulos G, Neufeld EF. Canine alpha-L-iduronidase deficiency. A model of mucopolysaccharidosis I. Am. J. Pathol. 1982; 109:244–248. [PubMed: 6215865]

Sloane Ja FAU, Batt CF, Ma YF, Harris Zm FAU, Trapp BF, Vartanian T. Hyaluronan blocks oligodendrocyte progenitor maturation and remyelination through TLR2. Proc Natl Acad Sci U S A. 2010; 107:11555–11560. [PubMed: 20534434]

Song S-K, Sun S-W, Ramsbottom MJ, Chang C, Russell J, Cross AH. Dysmyelination revealed through mri as increased radial (but unchanged axial) diffusion of water. Neuroimage. 2002; 17:1429–1436. doi:http://dx.doi.org/10.1006/nimg.2002.1267. [PubMed: 12414282]

Vite CH, Nestrasil I, Mlikotic A, Jens JK, Snella EM, Gross W, Shapiro EG, Kovac V, Provenzale JM, Chen S, Le SQ, Kan S-H, Banakar S, Wang RY, Haskins ME, Ellinwood NM, Dickson PI. Features of brain MRI in dogs with treated and untreated mucopolysaccharidosis type I. Comp. Med. 2013; 63:163–173. [PubMed: 23582423]

Wang RY, Aminian A, McEntee MF, Kan S-H, Simonaro CM, Lamanna W, Lawrence R, Ellinwood NM, Guerra C, Le SQ, Dickson PI, Esko JD. Intra-articular enzyme replacement therapy with rhIDUA is safe, well-tolerated, and reduces articular GAG Storage in the canine model of mucopolysaccharidosis type I. Mol. Genet. Metab. 2014:1–8.

Wei PT, Leong D, Calabrese E, White L, Pierce T, Platt S, Provenzale J. Diffusion tensor imaging of neural tissue organization: correlations between radiologic and histologic parameters. Neuroradiol. J. 2013; 26:501–510. [PubMed: 24199809]

Welti R, Mui E, Sparks A, Wernimont S, Isaac G, Kirisits M, Roth M, Roberts CW, Botté C, Maréchal E, McLeod R. Lipidomic analysis of Toxoplasma gondii reveals unusual polar lipids. Biochemistry. 2007; 46:13882–13890. [PubMed: 17988103]

Zimmerman RD, Fleming CA, Lee BC, Saint-Louis LA, Deck MD. Periventricular hyperintensity as seen by magnetic resonance: prevalence and significance. Am. J. Roentgenol. 1986; 146:443–450. [PubMed: 3484859]

Highlights

- We performed DTI of the brain in canine MPS I
- DTI suggested abnormal myelination in the corpus callosum of MPS I dogs
- Myelin composition was abnormal in MPS I corpus callosum
- There was a linear relationship between DTI metrics and myelin basic protein
- Abnormal myelination showed a response to treatment

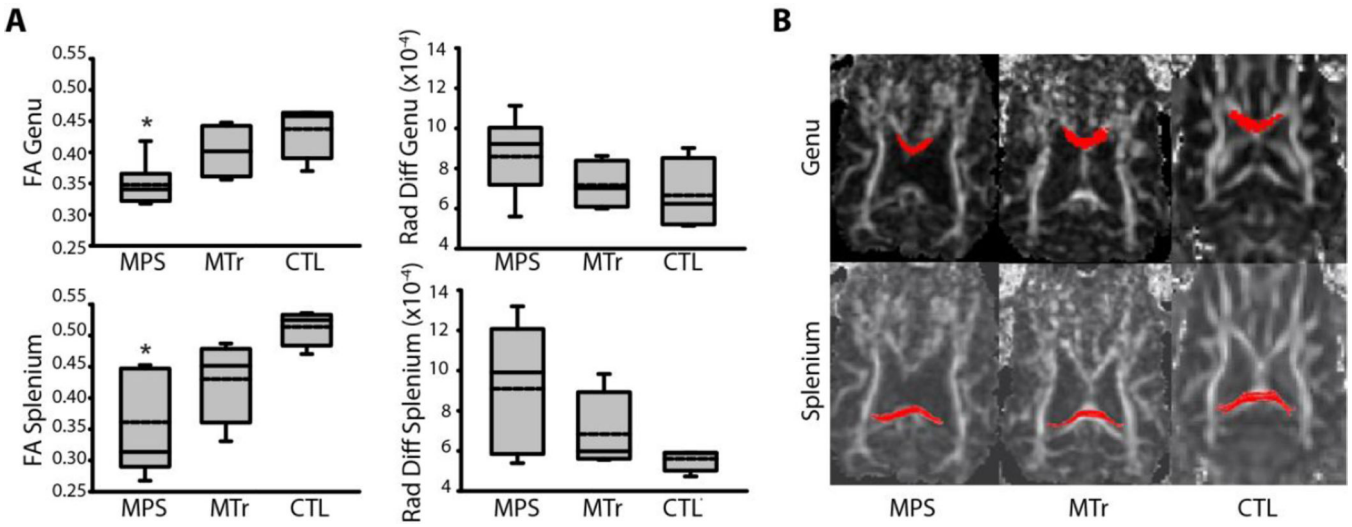

Fig. 1.

DTI of the corpus callosum. (**A**) Box plots of fractional anisotropy (FA) and radial diffusivity (Rad Diff) in the corpus callosum of untreated MPS I (MPS); MPS I dogs treated with intrathecal recombinant human alpha-L-iduronidase from age 4–21m (MTr); and unaffected heterozygote controls (CTL). Solid lines (the middle, lower and upper horizontal lines of the box) depict the median, 25th and 75th percentiles. Whiskers (the vertical lines and caps extending from the boxes) show the 10th and 90th percentiles. Dashed lines inside the boxes show the arithmetic means. ***P* < 0.01 vs. CTL. (**B**) Diffusion-weighted axial MR images illustrating the regions of interest that we used for tractography. The red color depicts regions corresponding to the genu (top panels) and splenium (lower panels) of the corpus callosum.

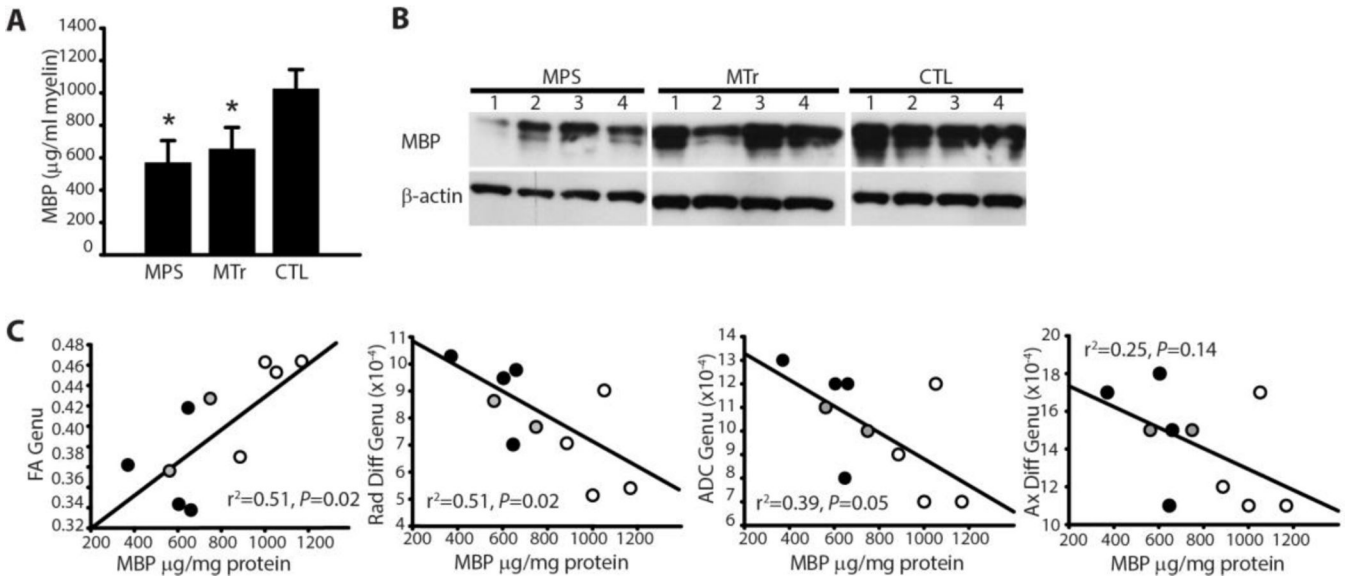

Fig. 2.

Myelin basic protein and relationship to DTI metrics. (**A**) Bar graph showing mean ± SD of myelin basic protein of myelin extracted from untreated MPS I (MPS), treated MPS I (MTr) and untreated heterozygous control dogs (CTL) per ml of extracted myelin. **P* < 0.05 vs. CTL. Values for genu and splenium from each dog were averaged. (**B**) Western blot of myelin basic protein (MBP) in myelin extracted from the corpus callosum. Numbers 1–4 correspond to MPS1, MPS2, etc. dogs in Fig. 4. β-actin is shown as a control. (**C**) Scatterplots showing fractional anisotropy (FA), radial diffusivity (Rad Diff), apparent diffusion coefficient (ADC) and axial diffusivity (Ax Diff) of the genu of the corpus callosum measured by DTI vs. MBP quantified from extracted myelin in MPS (black circles), MTr (gray circles), and CTL (open circles) dogs. Linear regression was performed with MBP as the dependent variable.

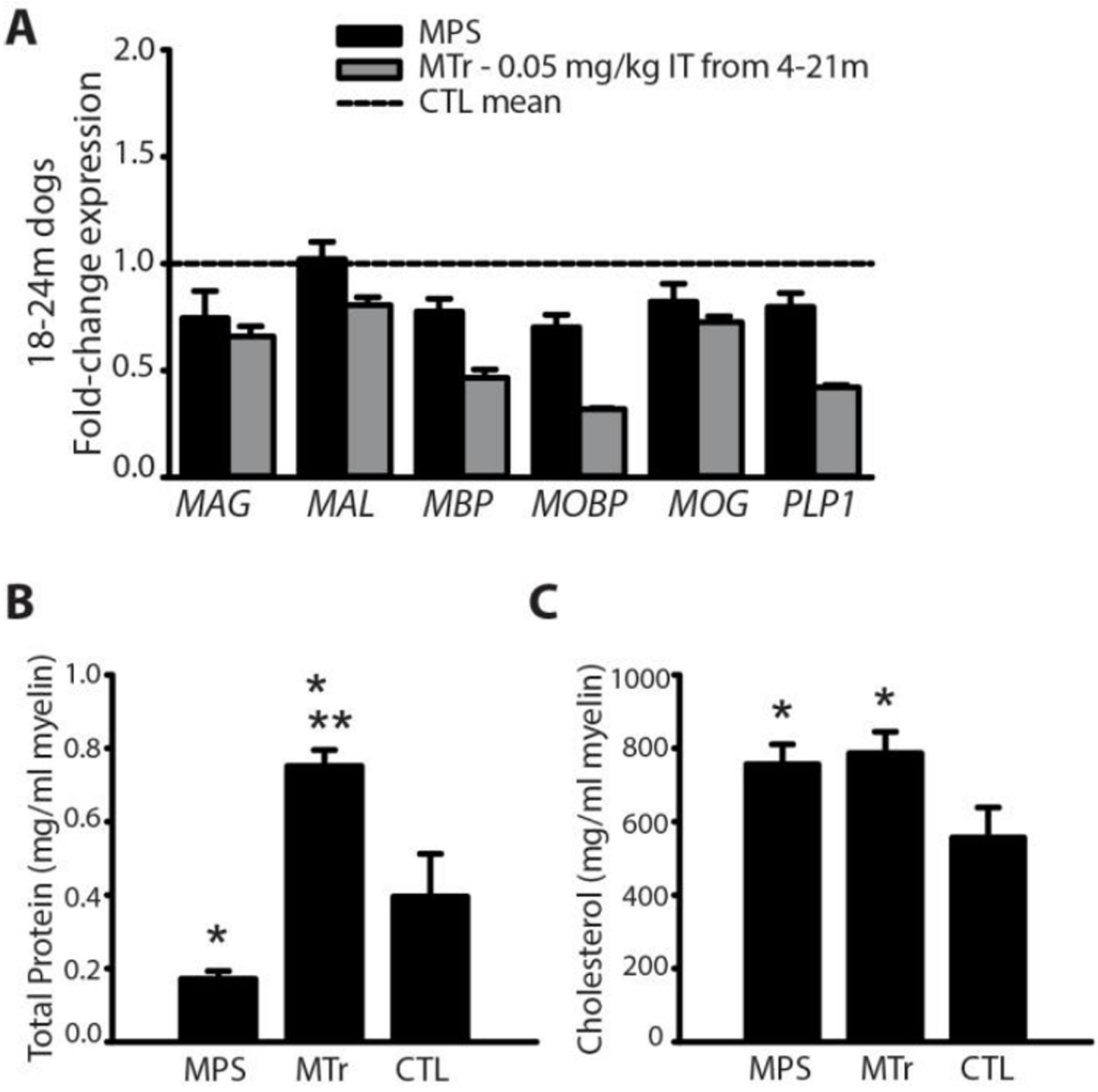

Fig. 3.

Myelin gene expression and composition. (**A**) RT-PCR of myelin-related genes in MPS dogs (n = 4), MTr dogs treated with IT recombinant human alpha-L-iduronidase from age 4–21m (n = 4), and CTL dogs (n = 4). (**B, C**) Bar graphs showing mean ± SD of total protein (**B**) and total cholesterol (**C**) of myelin extracted from the corpus callosum of untreated MPS I (MPS), treated MPS I (MTr) and untreated heterozygous control dogs (CTL) per ml of extracted myelin. Extracted myelin was normalized to volume (for protein), or to protein (for cholesterol). *P < 0.05 vs. CTL. **P < 0.05 vs. MPS. Values for genu and splenium from each dog were averaged.

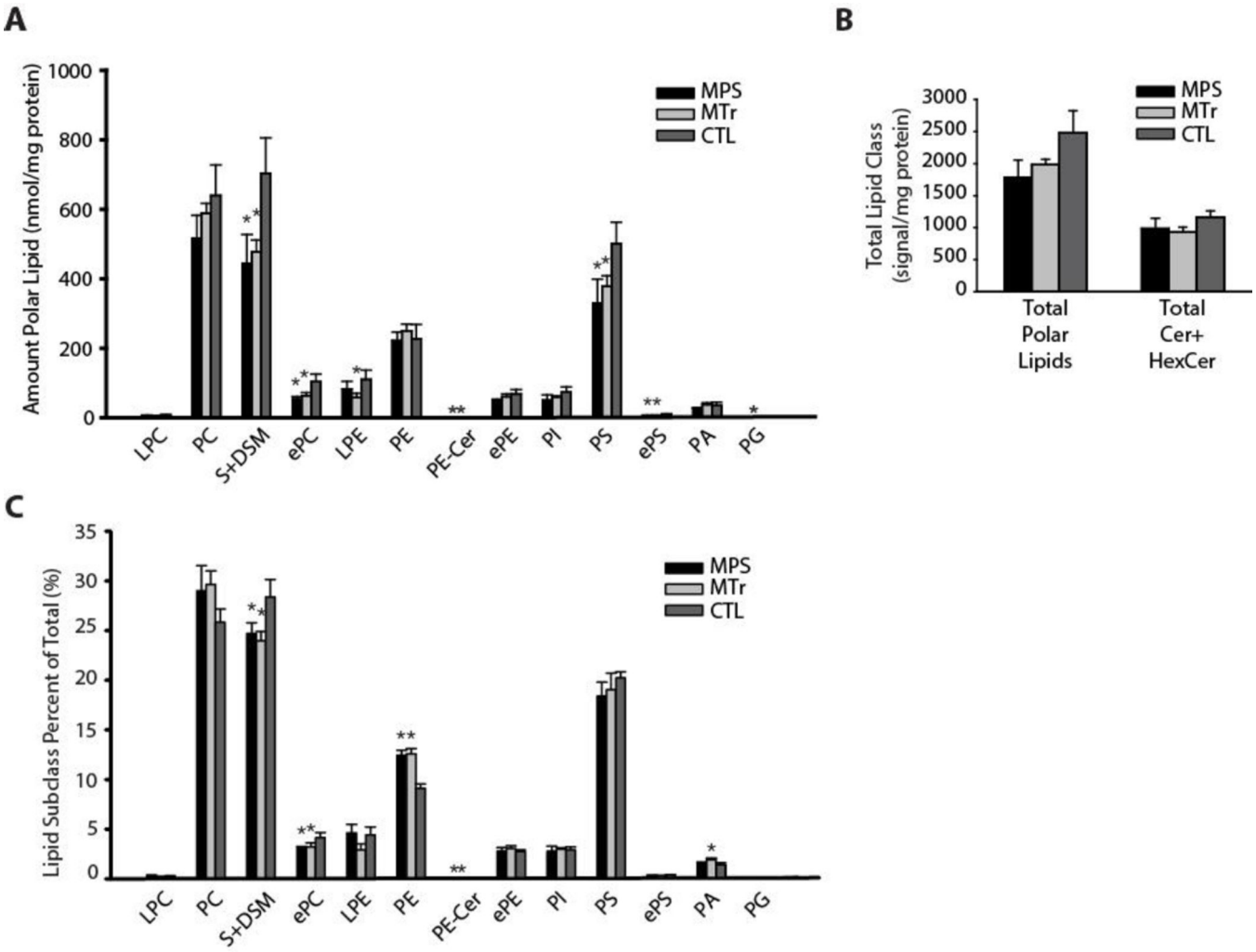

Fig. 4.

Lipidomic analysis of myelin phospholipids, and ceramides and hexosylceramides. (**A**) Total polar lipids by class. MPS, untreated MPS I; MTr, MPS I treated; CTL, carrier control. S, sphingomyelin; DSM, dihydrosphingomyelin; e, ether-linked (plasmalogen); PC, phosphatidylcholine; PS, phosphatidylserine; PE, phosphatidylethanolamine; L, lyso; Cer, ceramides; Hex, hexosyl. (**B**) Overall total polar lipid content. (**C**) Analysis by lipid class percent of total showing the composition of polar lipids.

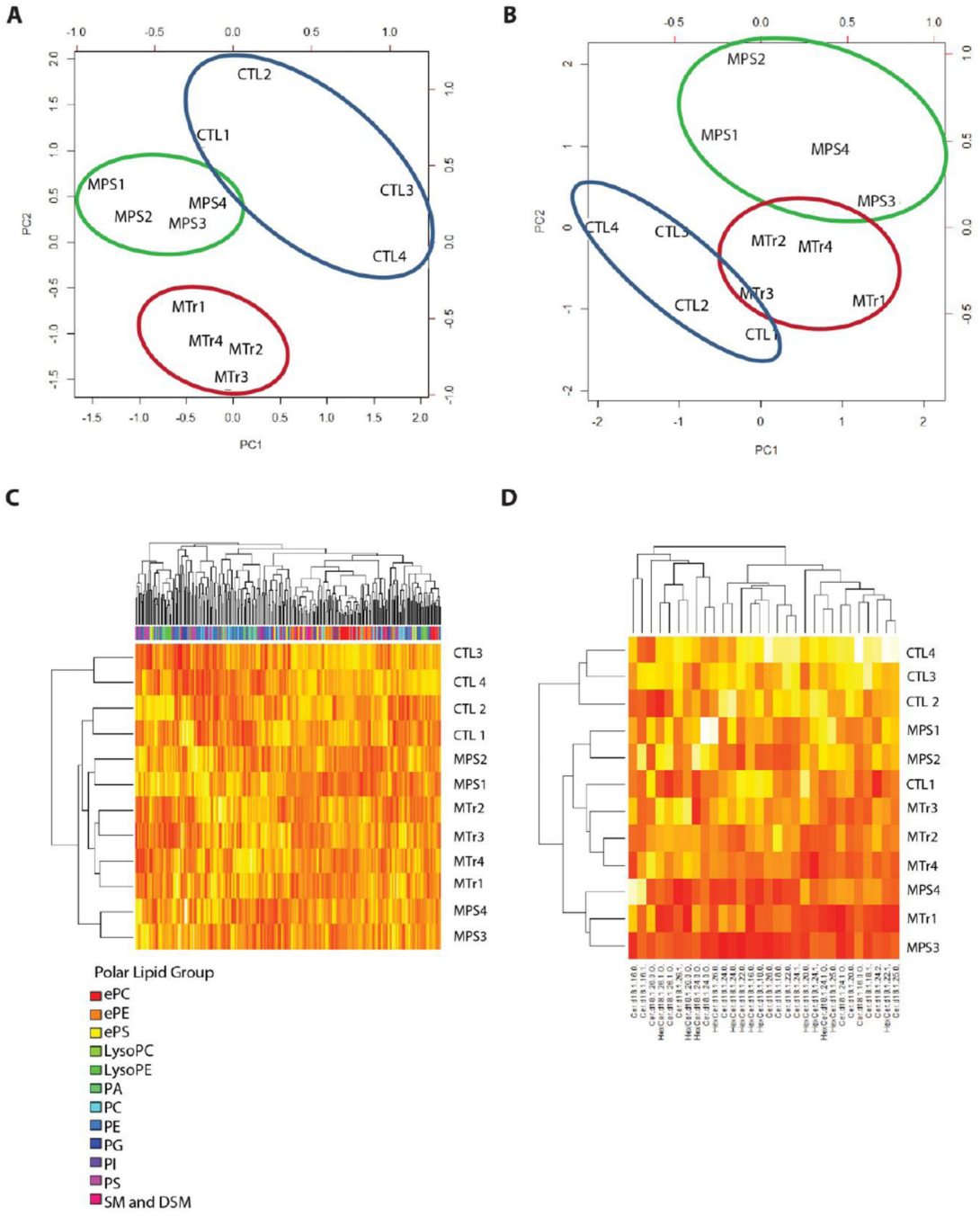

Fig. 5.

Principal components analysis and hierarchical clustering of myelin lipids. (**A**) Principal components analysis (PCA) by polar lipid species. (**B**) PCA by Cer + HexCer species. (**C**) Heatmap with hierarchical clustering by polar lipid species demonstrating overlap between MPS and MTr. White, highly positive, and red, negative, for standardized lipid values. (**D**) Heatmap, with hierarchical clustering by Cer + HexCer species.

Table 1

Canine subjects used in the study. The “X” marks studies in which a particular dog was included.

Subject	Group	DTI	RT-PCR	Myelin composition	Age at Necropsy
I-319	CTL	X	X	X	19 m
I-318	CTL	X	X	X	19 m
B-301	CTL	X	X	X	30 m
I-262	CTL	X	X	X	29 m
I-371*	MPS	X	X		20 m
I-388*	MPS	X	X		17 m
I-392*	MPS	X	X		17 m
I-393*	MPS	X	X		17 m
I-399	MPS	X			21 m
I-272	MPS	X	X	X	25 m
I-266	MPS	X	X	X	25 m
I-267	MPS	X	X	X	26 m
I-265	MPS	X	X	X	26 m
I-394	MTr	X	X	X	21 m
I-400	MTr	X	X	X	21 m
I-402	MTr	X	X	X	21 m
I-413	MTr	X	X	X	21 m

MPS: mucopolysaccharidosis; MTr: MPS I dogs treated with intrathecal recombinant human alpha-L-iduronidase; DTI: diffusion tensor imaging; RT-PCR: reverse transcriptase-polymerase chain reaction.

Dogs that received intra-articular alpha-L-iduronidase are marked with an *.

Table 2

DTI of the genu and splenium of the corpus callosum in heterozygous dogs (i.e., control, or CTL) dogs (n = 4), untreated dogs affected with mucopolysaccharidosis type I (MPS, n = 9) and MPS I dogs treated with intrathecal recombinant human alpha-L-iduronidase every three months from age 4m to 21m (MTr, n = 4). Metrics included fractional anisotropy (FA), apparent diffusion coefficient (ADC), axial diffusivity (Ax Diff), and radial diffusivity (Rad Diff). Each dog was scanned twice and the results averaged. Data are expressed as means of the means for each animal ± SD. Statistical analysis was performed using ANOVA with Tukey posthoc test.

	FA	ADC	Ax Diff	Rad Diff
Genu				
CTL	0.437 ± 0.0453	$8.74\ 10^{-4} \pm 2.18\times10^{-4}$	$1.29\times10^{-3} \pm 3.01\times10^{-4}$	$6.66\times10^{-4} \pm 1.79\times10^{-4}$
MPS	**0.348 ± 0.0318***	$1.05\times10^{-3} \pm 2.25\times10^{-4}$	$1.44\times10^{-3} \pm 3.23\times10^{-4}$	$8.60\times10^{-4} \pm 1.80\times10^{-4}$
MTr	0.402 ± 0.0428	$9.18\times10^{-4} \pm 1.31\times10^{-4}$	$1.32\times10^{-3} \pm 1.63\times10^{-4}$	$7.17\times10^{-4} \pm 1.21\times10^{-4}$
Splenium				
CTL	0.514 ± 0.0295	$8.29\times10^{-4} \pm 6.68\times10^{-5}$	$1.37\times10^{-3} \pm 1.04\times10^{-4}$	$5.60\times10^{-4} \pm 5.83\times10^{-5}$
MPS	**0.361 ± 0.0812***	$1.12\times10^{-3} \pm 3.20\times10^{-4}$	$1.55\times10^{-3} \pm 3.17\times10^{-4}$	$9.10\times10^{-4} \pm 3.22\times10^{-4}$
MTr	0.430 ± 0.0685	$9.12\times10^{-4} \pm 1.92\times10^{-4}$	$1.37\times10^{-3} \pm 1.87\times10^{-4}$	$6.84\times10^{-4} \pm 2.01\times10^{-4}$

*$P < 0.05$ versus CTL (bold type).

Table 3

Select polar lipid species from myelin extracted from the corpus callosum of heterozygous dogs (CTL, $n = 4$), untreated dogs affected with mucopolysaccharidosis type I (MPS, $n = 4$) and MPS I dogs treated with recombinant human alpha-L-iduronidase into the cerebrospinal fluid every three months from age 4m to 21m (MTr, $N = 4$). Data are expressed as mean ± SD nmol/mg protein. PC, phosphatidylcholine; SM, sphingomyelin; DSM, dihydrosphingomyelin; PS, phosphatidylserine; PI, phosphatidylinositol; PA, phosphatidic acid; e, ether-linked. (**A**) Polar lipid species that were low in affected dogs despite treatment ($P < 0.05$ for overall ANOVA, and Bonferroni-adjusted $P < 0.05$ for t-tests comparing CTL vs. MPS and CTL vs. MTr). SM, ePC, PS, and ePS species comprise the majority. Only one PC species remained significantly low with treatment. (**B**) Polar lipid species that were low in MPS, but were not significantly low in MTr dogs ($P < 0.05$ for overall ANOVA, and Bonferroni-adjusted $P < 0.05$ for t-test comparing CTL vs. MPS, and no significant difference between CTL vs. MTr).

(A) Species significantly low in affected dogs even with treatment				(B) Species low in affected dogs, but improved (not significantly low) with treatment			
	CTL	**MPS**	**MTr**		**CTL**	**MPS I**	**MTr**
PC 34:4	0.0792 ± 0.0417	0.0134 ± 0.0090	0.0250 ± 0.0096	PC 36:1	147.2 ± 22.0	96.3 ± 16.0	127.3 ± 3.3
SM 22:0	30.0 ± 8.6	9.9 ± 4.1	13.8 ± 5.1	PC 38:3	4.19 ± 0.48	3.25 ± 0.36	4.13 ± 0.19
SM 24:0	152 ± 30	90 ± 16	94 ± 5	PC 40:2	5.95 ± 0.79	4.23 ± 0.98	4.72 ± 0.43
SM 24:1	294 ± 33	192 ± 31	185 ± 15	PC 42:11	0.154 ± 0.050	0.045 ± 0.021	0.096 ± 0.060
ePC 34:2	8.37 ± 1.75	3.87 ± 0.58	5.10 ± 1.56	DSM 16:0	2.59 ± 1.06	0.862 ± 0.203	1.93 ± 0.47
ePC 34:1	30.5 ± 8.3	15.8 ± 1.8	18.2 ± 4.1	SM 22:1	25.4 ± 6.4	13.2 ± 1.5	16.9 ± 2.9
ePC 36:3	7.88 ± 2.16	3.37 ± 0.45	4.69 ± 0.61	ePC 32:2	0.238 ± 0.042	0.097 ± 0.048	0.238 ± 0.060
ePC 36:2	8.67 ± 2.05	3.97 ± 0.73	4.98 ± 0.48	ePC 32:1	3.18 ± 0.57	1.88 ± 0.31	2.40 ± 0.55
ePC 36:1	10.21 ± 1.32	6.28 ± 0.81	7.19 ± 0.04	ePC 36:4	1.51 ± 0.64	0.62 ± 0.05	1.0 ± 0.2
ePC 38:3	1.61 ± 0.39	0.70 ± 0.23	0.84 ± 0.08	ePC 38:4	1.38 ± 0.48	0.71 ± 0.03	0.84 ± 0.12
ePC 38:2	4.11 ± 0.62	2.25 ± 0.39	2.47 ± 0.24	PE 38:0/ePE 40:7	1.30 ± 0.31	0.826 ± 0.216	1.25 ± 0.09
ePC 38:1	5.90 ± 0.28	3.30 ± 0.65	3.60 ± 0.28	ePE 34:2	4.69 ± 0.76	3.01 ± 0.38	3.96 ± 0.81
ePC 40:3	0.892 ± 0.254	0.436 ± 0.106	0.508 ± 0.084	ePE 36:5	0.292 ± 0.119	0.119 ± 0.021	0.246 ± 0.061
ePC 40:2	5.65 ± 0.16	3.59 ± 0.53	3.33 ± 0.59	ePE 36:3	10.6 ± 0.9	6.7 ± 0.9	8.9 ± 1.7
PS 36:1	317 ± 37	193 ± 44	228 ± 20	ePE 36:2	3.60 ± 0.71	2.37 ± 0.27	2.85 ± 0.22
PS 38:2	15.8 ± 3.3	9.4 ± 2.0	10.2 ± 0.6	ePE 38:3	3.72 ± 0.33	2.38 ± 0.31	2.84 ± 0.65
PS 38:1	14.2 ± 2.6	7.4 ± 1.2	7.1 ± 1.2	PI 34:1	4.08 ± 1.17	2.07 ± 0.68	2.84 ± 0.40
PS 40:8	0.521 ± 0.060	0.227 ± 0.119	0.254 ± 0.104	PI 36:1	2.25 ± 0.60	1.00 ± 0.37	1.84 ± 0.49
PS 40:2	4.21 ± 0.99	2.67 ± 0.58	2.48 ± 0.20	PS 36:2	38.4 ± 6.2	25.5 ± 6.6	27.6 ± 2.1

(A) Species significantly low in affected dogs even with treatment				(B) Species low in affected dogs, but improved (not significantly low) with treatment			
	CTL	**MPS**	**MTr**		**CTL**	**MPS I**	**MTr**
PS 40:1	2.93 ± 0.53	1.39 ± 0.13	1.37 ± 0.20	PS 42:11	0.279 ± 0.042	0.104 ± 0.069	0.200 ± 0.053
PS 42:8	0.704 ± 0.085	0.412 ± 0.097	0.383 ± 0.056	PA 36:3	0.667 ± 0.064	0.481 ± 0.079	0.779 ± 0.052
ePS 38:2	1.24 ± 0.19	0.69 ± 0.21	0.67 ± 0.10	ePS 36:1	2.70 ± 0.22	1.74 ± 0.47	2.06 ± 0.22
ePS 38:1	2.94 ± 0.56	1.74 ± 0.36	1.57 ± 0.34	ePS 38:6	0.38 ± 0.04	0.15 ± 0.10	0.34 ± 0.07
ePS 40:2	0.658 ± 0.148	0.310 ± 0.130	0.375 ± 0.032	ePS 38:3	0.18 ± 0.03	0.08 ± 0.05	0.14 ± 0.04

Note: Although species in panel B may be considered improved as defined by statistical testing, the degree of improvement in many species still appears incomplete.

Table 4

Ceramides (Cer) and Hexosylceramides (HexCer) from myelin extracted from the corpus callosum of heterozygous dogs (CTL, *n* = 4), untreated dogs affected with mucopolysaccharidosis type I (MPS, *n*=4) and MPS I dogs treated with recombinant human alpha-L-iduronidase into the cerebrospinal fluid every three months from age 4m to 21m (MTr, *n* = 4). Data are presented as mean ± SD signal/mg protein.

	CTL	MPS	MTr
Cer-D18:1(16:0)	0.588 ± 0.085	0.624 ± 0.218	0.581 ± 0.127
Cer-D18:1(16:0-O)	0.679 ± 0.534	0.170 ± 0.036	0.0679 ± 0.0534
Cer-D18:1(18:0)	8.38 ± 1.34	**5.53 ± 0.84***	7.49 ± 1.14
Cer-D18:1(18:1)	1.25 ± 0.28	1.03 ± 0.14	0.98 ± 0.10
Cer-D18:1(20:0)	1.59 ± 0.13	**1.21 ± 0.20***	**1.03 ± 0.05****
Cer-D18:1(22:0)	3.20 ± 0.74	**1.82 ± 0.18***	2.50 ± 0.14
Cer-D18:1(24:0)	14.5 ± 1.6	**10.3 ± 1.5***	13.0 ± 1.1
Cer-D18:1(24:1)	40.9 ± 5.2	**29.6 ± 1.60***	**32.2 ± 2.9****
Cer-D18:1(24:1-O)	6.71 ± 0.64	5.88 ± 0.98	5.43 ± 0.84
Cer-D18:1(24:2)	2.05 ± 0.52	1.92 ± 0.26	1.83 ± 0.29
Cer-D18:1(26:0)	2.40 ± 0.29	1.98 ± 0.24	2.09 ± 0.09
Cer-D18:1(26:1)	5.04 ± 0.80	3.82 ± 0.52	4.78 ± 0.75
Cer-D18:1(25:0)	5.25 ± 0.73	4.71 ± 0.49	4.25 ± 0.39
Cer-D18:1(24:0-O)	3.84 ± 0.24	4.18 ± 1.01	3.69 ± 0.07
Cer-D18:1(26:1-O)	1.60 ± 0.28	1.69 ± 0.33	1.59 ± 0.24
Cer-D18:1(26:0-O)	0.29 ± 0.11	0.25 ± 0.08	0.33 ± 0.07
Hexcer-D18:1(16:0)	2.20 ± 0.15	1.73 ± 0.32	1.74 ± 0.28
Hexcer-D18:1(18:0)	69.6 ± 10.3	**46.0 ± 10.7***	57.5 ± 9.5
Hexcer-D18:1(20:0)	14.3 ± 2.9	12.1 ± 2.6	10.4 ± 2.5
Hexcer-D18:1(22:0)	42.4 ± 3.7	**27.6 ± 5.1***	35.5 ± 6.1
Hexcer-D18:1(22:1)	26.8 ± 5.6	23.5 ± 3.72	21.3 ± 3.0
Hexcer-D18:1(24:1)	411 ± 47	344 ± 47	**288 ± 52****
Hexcer-D18:1(24:1-O)	34.8 ± 5.5	33.8 ± 6.5	26.3 ± 2.1
Hexcer-D18:1(24:0)	199 ± 26	157 ± 36	166 ± 13
Hexcer-D18:1(24:0-O)	85.7 ± 16.3	95.3 ± 24.8	88.3 ± 18.2
Hexcer-D18:1(26:0)	22.5 ± 1.8	22.6 ± 6.1	21.6 ± 2.0
Hexcer-D18:1(25:0)	103 ± 13	103 ± 19	78.3 ± 7.3
Hexcer-D18:1(26:1-O)	7.88 ± 1.81	8.04 ± 1.14	8.31 ± 1.68
Hexcer-D18:1(26:0-O)	41.7 ± 4.8	35.5 ± 7.5	42.1 ± 13.2

*$P < 0.05$ for MPS vs CTL and **$P < 0.05$ for MPS vs MTr. P-values are Bonferroni-adjusted.

Bold type with * or ** indicates statistical significance.